RSC Advances

PAPER

View Article Online
View Journal | View Issue

Check for updates

Cite this: *RSC Adv.*, 2020, **10**, 21481

Electron beam irradiation influencing the mechanical properties and water absorption of polycaprolactam (PA6) and polyhexamethylene adipamide (PA66)

Juan Wang,[a] Jianping Qiu,[b] Siyi Xu,*[d] Jianxi Li*[c] and Liguo Shen [d]

It is known that polycaprolactam (PA6) and polyhexamethylene adipamide (PA66) are widely used industrial materials including in the irradiation industry. However, there is a lack of observation of irradiation effects on PA6 and PA66. In the current study, we firstly investigated mechanical and water absorption properties of PA6 and PA6 that were treated under irradiation doses of 200 kGy, 400 kGy, 800 kGy and 1600 kGy, respectively. The structure, mechanical properties and thermal properties of nylon after irradiation were characterized by mechanical property tests, Fourier transform infrared spectroscopy (FTIR) and scanning electron microscopy (SEM). The results indicated that the tensile strength of PA6 increased gradually while that of PA66 firstly increased and then decreased with the increase of irradiation dose. Additionally, the elongation at break of the two samples decreased obviously with the increase of irradiation dose. The water absorption of PA6 increased with the increase of irradiation dose; however, that of PA66 was almost constant regardless of irradiation. FTIR tests revealed that the carbonyl index of PA6 and PA66 increased with the increase of irradiation dose. SEM results illustrated that surface degradation of PA6 and PA66 occurred during the irradiation process.

Received 24th April 2020
Accepted 25th May 2020

DOI: 10.1039/d0ra03673k

rsc.li/rsc-advances

Open Access Article. Published on 05 June 2020. Downloaded on 12/4/2025 11:48:17 PM.
This article is licensed under a Creative Commons Attribution-NonCommercial 3.0 Unported Licence.

1. Introduction

As the most commonly used thermoplastic resins, polyamides are widely used in many fields including textiles, automobiles and medical equipment,[1–4] while the main product is short chain nylon, including polycaprolactam (PA6) and polyhexamethylene adipamide (PA66).[5–7] The melting point of PA is very high due to hydrogen bonding. The melting point of PA66 can reach about 260 °C; however, the continuous operating temperature of PA is not high and it easily absorbs water.[8–11] The segmental structures of PA6 and PA66 are similar. As there is only nuance between their microstructures, the effects of their intermolecular hydrogen bonding are not obviously different. There are more hydrogen bonds in the molecular chain of PA66. It shows stronger intermolecular interactions and better thermodynamic stability than PA6. However, PA6 demonstrates excellent molding processability, water absorption property, thermal stability, weather resistance comparing to PA66, however, its melting point is lower.[12,13]

It is generally known that the irradiation effect will result in crosslinking, cleavage and grafting of polymers. Therefore, electron beam irradiation technology has been widely used in the modifications of polymers.[14–16] Sengupta and co-workers[17] prepared PA66 film by slice compression molding method and then studied the performances of the sample after irradiation. It was found in the experiment that the crystallinity of the PA film after irradiation initially decreased rapidly with the increase of the irradiation dose and then the decreasing speed slowed down. Adem and co-workers[18] found that crosslinking and cleavage of the chain occurred simultaneously during irradiation. The melting and crystallization temperatures of the film both decreased with the increase of the irradiation dose. The fracture stress and strain decreased rapidly, while the elastic modulus and the yield stress increased significantly. Jung and co-workers[19] studied the effects of electron beam irradiation on the structure and mechanical properties of nylon 66 fiber. It was found that the irradiation mainly caused the oxidative degradation of molecular chain of the nylon 66 and lowered the thermal stability of the nylon material, resulting in micro cracks and significant stress concentration effects, which severely damaged the mechanical properties of the material. Aden and co-workers[20] studied the PA66/PP blending system with enhanced compatibility by electron beam irradiation in terms of microstructure and mechanical properties. The study showed that the compatibility of PA and PP was increased by the

[a]Jinhua Huanke Environmental Technology Co., Ltd., Jinhua 321000, China. E-mail: 719117808@qq.com
[b]Jinhua Polytechnic, Jinhua 321007, China. E-mail: jianpingqiu@jhc.edu.cn
[c]CGN DELTA Jiangsu Plast & Chem Co., Ltd., Suzhou 215400, P. R. China. E-mail: 570800202@qq.com
[d]Zhejiang Normal Univ., Coll. Geog. & Environm. Sci., Jinhua 321004, P. R. China. E-mail: 601518368@qq.com; lgshen@zjnu.cn

Open Access Article. Published on 05 June 2020. Downloaded on 12/4/2025 11:48:17 PM.
This article is licensed under a Creative Commons Attribution-NonCommercial 3.0 Unported Licence.

irradiation system which provided a new strategy for manufacture and structural properties control of high-performance PA66/PP blend alloy. With the continuous development of high-energy irradiation technology,[21–26] its advantages of high efficiency, cleanliness and easy control are widely favored. Electron beam irradiation and other energy irradiations are gradually used in industrial productions. When a linear polymer turns to three-dimensional structure by irradiation crosslinking, some changes will happen to its physical properties, chemical properties, heat resistance and flame retardancy. Therefore, irradiation crosslinking is regarded as an effective method to optimize polymer performances.[27,28] However, the effects of radiation on PA are still fuzzy and need a significant observation. This is highly desired if the PA materials are used in the field of nuclear power, nuclear power insulation devices and cable jackets.

In this study, PA6 and PA66 are used and investigated by mechanical tests and water absorption tests after adopting different doses of electron beam irradiation. It is expected to discover the rule of effects of irradiation on the performances of PA6 and PA66 as well as provide guidance for the wide use of nylon products in the field of nuclear power, especially nuclear power insulation devices and cable jackets.

2. Experimental

2.1. Main raw materials and equipment

Nylon 6, T28 and nylon 66, 4820, molecular weight 15 000–33 000, injection molding grade, polymerization degree 150–300 (YSK, China). Injection molding machine, HY-126N-B (HY Instrument, China). Shore durometer, LX-D (HBO Instrument, China). Electronic balance (PRECISA, Switzerland). Microcomputer control electron universal testing machine, ETM-A (Wance, China). Fourier transform infrared spectrometer (FT-IR), Tensor II (Bruker, Germany). Scanning electron microscope (SEM), Phenom Pro (Phenom-World BV, Netherlands). Electron accelerator, 1.5 MeV (Chinese Academy of Sciences).

2.2. Experimental procedures

The samples used in this study are made by an injection molding machine and placed in a constant temperature and humidity room with a room temperature of 23 ± 2 °C and a humidity of 50% (±5) specified by GB/T1040.1-2018 for more than 10 hours. PA6 and PA66 were made into samples of different specifications according to the experimental needs by an injection molding machine. The injection pressure was 60 MPa. The tensile sample is prepared into a dumbbell shape, the total length, the width of the narrow part and the thickness are 150 mm, 10 mm and 4 mm according to GB/T1040.2-2006, respectively. The water absorption rate sample is prepared into a rectangular shape with length, width and height of 20 mm, 10 mm and 1 mm according to GB/T1034-2008. The samples were irradiated by electron beam with different irradiation doses. The irradiation doses were 0, 200, 400, 800 and 1600 kGy, respectively. The dose rate was 2.4×10^4 kGy h^{-1}.

2.3. Tests and characterizations

Mechanical properties. Elongations at break and tensile strengths of the samples were tested by tensile tests according to GB/T1040.2-2006. The elongation speed was 100 mm min^{-1}. FTIR analysis is similar with the previous reports.[29,30] Briefly, the sample was put on the FTIR spectrometer and reflection method was adopted for the tests. Scan range was 4000–600 cm^{-1}. Scan number was 32.

Morphology analysis. Surface of the sample was sprayed with gold and its cross section was observed by SEM, which is similar with the previous reports.[31,32] Accelerating voltage was 10 kV.

Water absorption test. The sample was immersed in water for 48 h at room temperature. Coefficient of water absorption (CWA) was calculated by the equation below:

$$\mathrm{CWA} = \frac{m_1 - m_0}{m_0} \times 100\% \quad (1)$$

In the equation, CWA is coefficient of water absorption (%), while m_0 is the mass before water absorption (g) and m_1 is the mass after water absorption (g).

2.4. Mechanical properties

Variation trends strengths and elongations at break of PA6 and PA66 under different irradiation doses are shown in Fig. 1 and 2. According to Fig. 1, with the increase in the irradiation dose, the fracture strength of PA6 gradually increases and the elongation at break continues to decrease, while rate of the decreasing obviously slows down when the irradiation dose exceeds 400 kGy. Molecular chain of PA6 is hardened through crosslinking when the irradiation dose gradually increases. Therefore, its tensile strength gradually increases. However, because the slip between the segments of the molecular chain is limited by the crosslinking network structure, the elongation at break decreases significantly. It is found from Fig. 2 that the tensile strength of PA66 increases at the beginning and then decreases, so that a peak at 400 kGy is reached, indicating that crosslinking mainly happens in the polymer when the irradiation dose is low. When the irradiation dose exceeds 400 kGy, the degradation process becomes more obvious and both of the

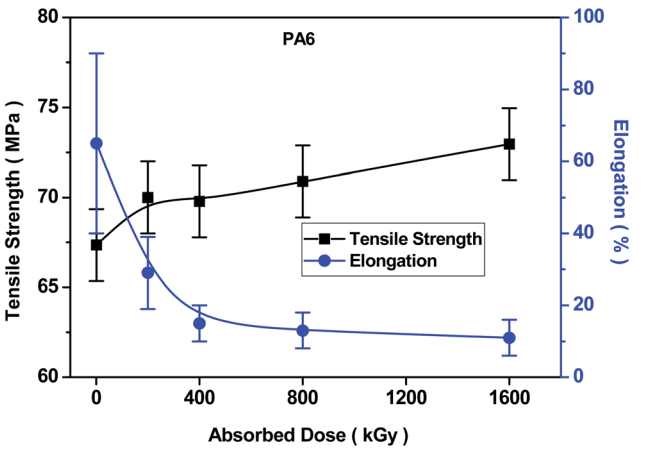

Fig. 1 Influences of irradiation dose on mechanical properties of PA6.

This journal is © The Royal Society of Chemistry 2020

Open Access Article. Published on 05 June 2020. Downloaded on 12/4/2025 11:48:17 PM.
This article is licensed under a Creative Commons Attribution-NonCommercial 3.0 Unported Licence.

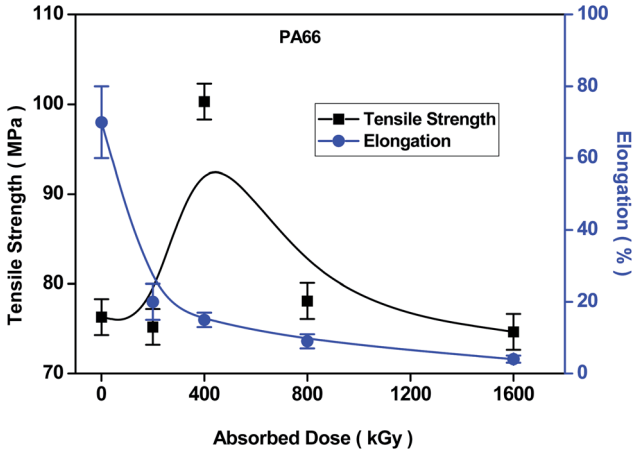

Fig. 2 Influences of irradiation dose on mechanical properties of PA66.

strength and tensile toughness of the material decrease rapidly. When the irradiation dose is 1600 kGy, the tensile strength of PA66 is the same as that without being irradiated, indicating that the effect of degradation process is not obvious and over crosslinking is dominant in the irradiation process at the same time.

2.5. Water absorption

Crosslinking improves not only thermal stability and mechanical properties, but also chemical resistance of materials and thus expands application scope of the materials. Variation trends of water absorptions of PA6 and PA66 under different irradiation doses are shown in Fig. 3. According to Fig. 3, water absorption of PA6 gradually increases with increase in the irradiation dose. The possible reason is that after the irradiation, slight degradation happens on the surface of PA6 and polar groups are formed such as carbonyl groups, carboxyl groups, ester groups and hydroxyl groups which improves the hydrophilicity of the material. Because most of these polar groups are generated on the surface of the material and their amounts are relatively less, the improvement of the hydrophilicity is limited.[33–36] The water absorption of PA66 is almost constant and remains about 3.1%, indicating that crosslinking is dominant on the surface of PA66 after the irradiation and the degradation is not significant.

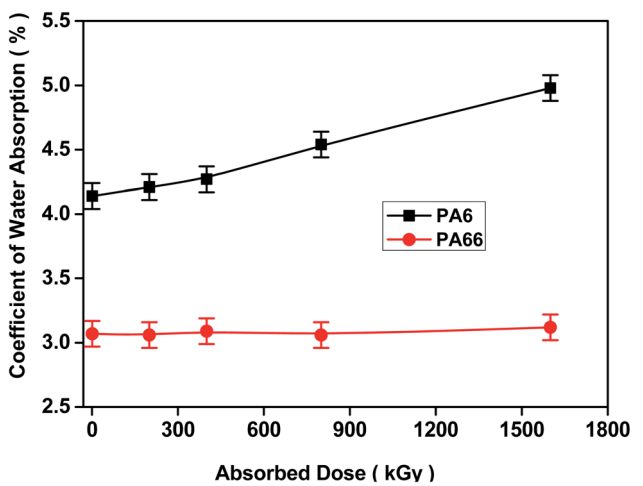

Fig. 3 Influences of irradiation dose on water absorption of samples.

2.6. FT-IR

The changes in microstructures of the PA materials under different irradiation doses are shown in Fig. 4. According to Fig. 4(a) and (b), characteristic peaks of amide I bond (stretching vibration of carbonyl group) and amide II bond (bending vibration of amino group) of PA6 and PA66 are indicated by the absorption peaks at 1650 cm^{-1} and 1540 cm^{-1}, respectively. The absorption peak at 3300 cm^{-1}, 2923 cm^{-1}, 2860 cm^{-1} and 1715 cm^{-1} are the stretching vibration peaks of the amino group, the methylene group, the methylene group and the carbonyl group of ketone compound, respectively.[37] The absorption peak at 1740 cm^{-1} is the stretching vibration peak of the carbonyl group affected by hydrogen bonding effect. It is found from the figure that the positions of the peaks of PA are not changed before and after the irradiation. However, intensities of the peaks at 1715 cm^{-1} and 1740 cm^{-1} continuously increase with the increase of absorbed dose. Carbonyl indices (R1745 and R1740, %) are defined as the ratio between the peak areas at 1715 cm^{-1} and 1740 cm^{-1} and the peak area at 2923 cm^{-1}, respectively. Calculations are based on formulas (2) and (3).

$$R_{1715} = \frac{H_{1715}}{H_{2923}} \times 100\% \quad (2)$$

$$R_{1740} = \frac{H_{1740}}{H_{2923}} \times 100\% \quad (3)$$

Curves of the carbonyl indices as a function of irradiation dose are shown in Fig. 4(c) and (d). It is found that the carbonyl index continue to increase with the increase of the irradiation dose. This is because that the electron beam irradiation in the air causes oxidation of surface of PA and then the concentration of carbonyl groups on the surface of the sample increases.[38–41] PA66 shows lower carbonyl index under the same irradiation dose, indicating that it is less affected by irradiation and its stability is better comparing to PA6.

2.7. Morphology

The variation trends of the surface morphology of PA under different irradiation doses are shown in Fig. 5. The surface pictures in Fig. 5 can obviously show an electron beam etching phenomenon and snowflake images. The more and more defects can give a rougher and rougher surface. This is because during the irradiation, the impact of the electron beam conducts etching effect on the surface of the material. The integrity of the surface of the material is damaged, resulting in the generation of free radicals on the surface of PA. Thus, oxidation reactions occur and the molecular backbone breaks,

Open Access Article. Published on 05 June 2020. Downloaded on 12/4/2025 11:48:17 PM.
This article is licensed under a Creative Commons Attribution-NonCommercial 3.0 Unported Licence.

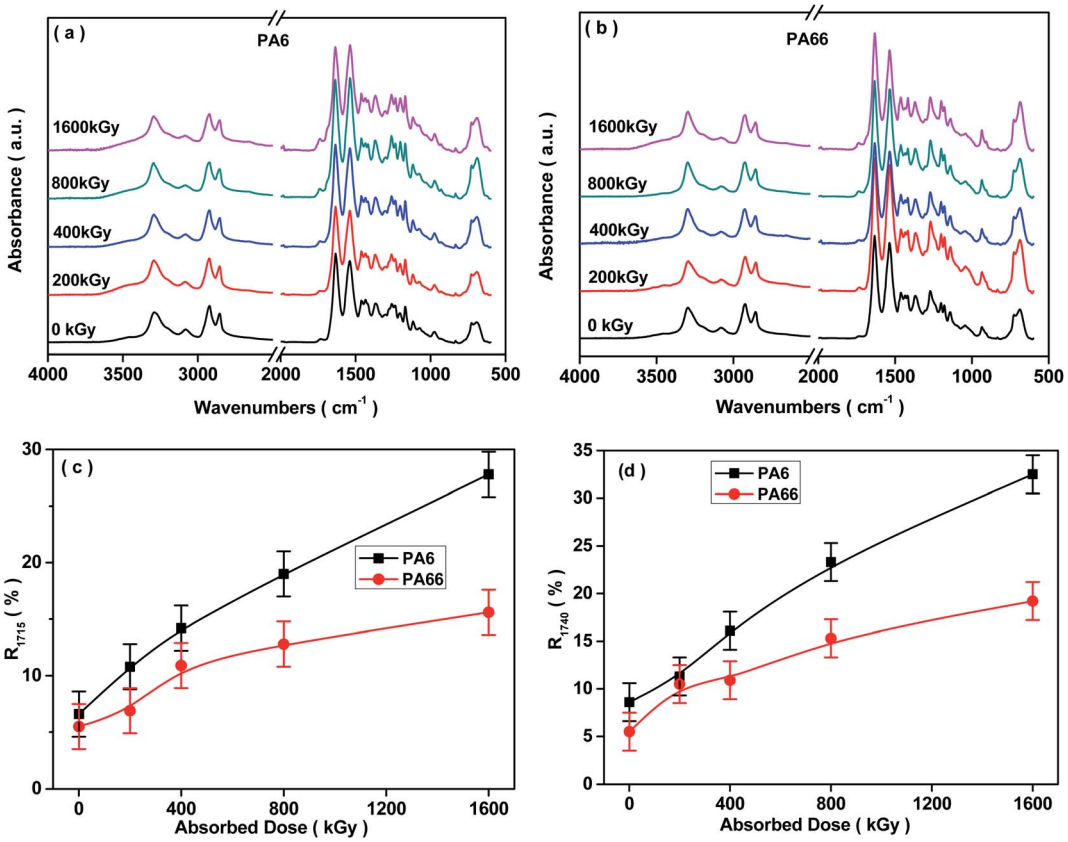

Fig. 4 Influences of irradiation dose on microstructures of samples (a and b) FTIR of PA6 and PA66; (c and d) carbonyl index of PA6 and PA66.

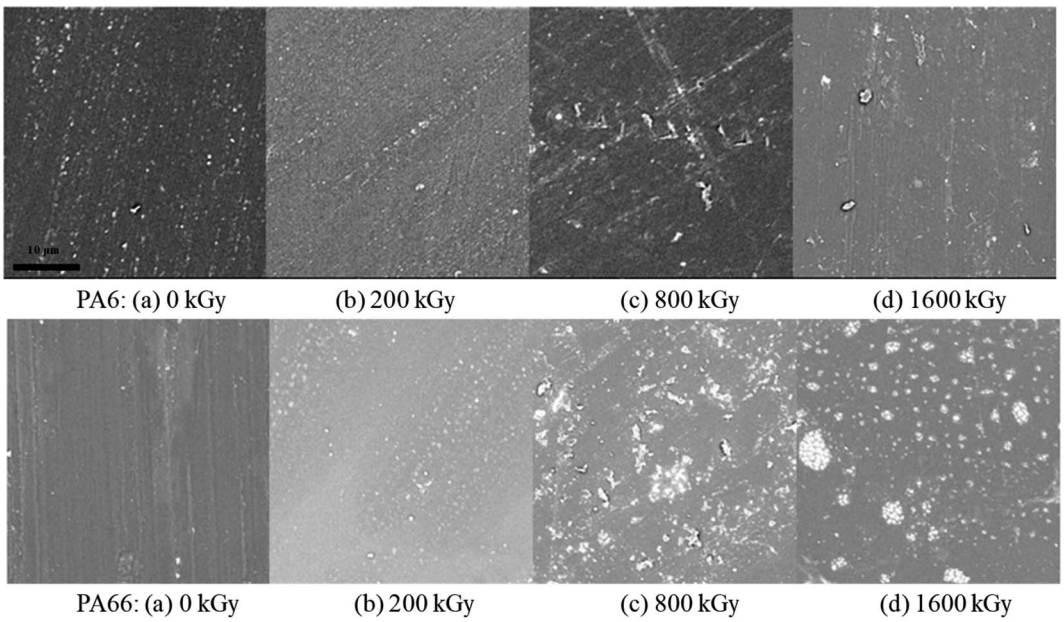

Fig. 5 Influences of irradiation dose on morphology of samples.

while the surface of the material is degraded and becomes rough.[42–44] In addition, the more intense oxidation reaction can make the surface rougher with the increase of the irradiation dose.

3. Conclusions

PA6 and PA66 were irradiated by electron beam. The influences of irradiation dose on properties of the samples were studied by

 This journal is © The Royal Society of Chemistry 2020

Open Access Article. Published on 05 June 2020. Downloaded on 12/4/2025 11:48:17 PM.
This article is licensed under a Creative Commons Attribution-NonCommercial 3.0 Unported Licence.

mechanical property tests, FT-IR, and SEM, *etc.* The results of mechanical property tests indicate that the elongations at break of PA6 and PA66 both reduces to below 10% with increase in the irradiation dose. Comparing to PA6, the maximum fracture strength of PA66 reaches 93 MPa after the irradiation. The strength is significantly improved. The results of water absorption tests show that the influences of irradiation effect on water absorption of PA66 is smaller than PA6. The results of FT-IR show that carbonyl index of PA6 and PA66 samples increases with increase in irradiation dose, indicating that surface oxidation of PA is resulted from the irradiation. The SEM results show that the surface of PA is rougher with increase in the irradiation dose, illustrating the surface degradation which is consistent with the FT-IR results. PA66 has a lower carbonyl index under the same irradiation dose compared with PA6, indicating that it is less affected by irradiation and more stable. This is mainly because PA66 contains more hydrogen bonds than PA6, and more energy is needed to break the hydrogen bond. These results was firstly found in this study and display a huge potential for the research and applications of PA66 and PA6 in various areas.

Conflicts of interest

The authors declare no conflict of interest.

Acknowledgements

This study was financially supported by Natural Science Foundation of Zhejiang Province (No. LQ15E080007).

References

1 F. Bondan, M. R. F. Soares and O. Bianchi, *Polym. Bull.*, 2014, **71**, 151–166.
2 O. Bianchi, A. J. Zattera and L. B. Canto, *J. Elastomers Plast.*, 2010, **42**, 561–575.
3 S. W. Hwang, S. W. Kim, H. Y. Park, I. L. Jeon and K. H. Seo, *J. Appl. Polym. Sci.*, 2011, **119**, 3136–3144.
4 S. Mani, P. Cassagnau, M. Bousmina and P. Chaumont, *Macromol. Mater. Eng.*, 2011, **296**, 909–920.
5 H. Liao, L. Zheng, Y. Hu, X. Zha, X. Xu, Y. Wen, G. Tao and C. Liu, *J. Appl. Polym. Sci.*, 2015, **132**, 42091.
6 J. Li, R. Y. Bao, W. Yang, B. H. Xie and M. B. Yang, *Mater. Des.*, 2012, **40**, 392–399.
7 F. M. Xiang, Y. Y. Shi, X. X. Li, T. Huang, C. Chen, Y. Peng and Y. Wang, *Eur. Polym. J.*, 2012, **48**, 350–361.
8 P. Y. Le Gac, M. Arhant, M. Le Gall and P. Davies, *Polym. Degrad. Stab.*, 2017, **137**, 272–280.
9 A. Hassan, N. M. Salleh, R. Yahya and M. R. K. Sheikh, *J. Reinf. Plast. Compos.*, 2011, **30**, 488–498.
10 E. E. Garcia, D. F. S. Freitas, S. P. Cestari, D. R. Coval, L. C. Mendes and G. A. V. Albitres, *J. Therm. Anal. Calorim.*, 2020, **139**, 293–303.
11 V. Miri, O. Persyn, J. M. Lefebvre and R. Seguela, *Eur. Polym. J.*, 2009, **45**, 757–762.
12 J. Huang, W. Ulrich, S. Schmauder and S. Geier, *Comput. Mater. Sci.*, 2011, **50**, 1315–1319.
13 M. Nase, B. Langer, S. Schumacher and W. Grellmann, *J. Appl. Polym. Sci.*, 2009, **111**, 2245–2252.
14 L. G. Shen, J. X. Li, R. J. Li, H. J. Lin, J. R. Chen and B. Q. Liao, *Appl. Surf. Sci.*, 2018, **437**, 75–81.
15 L. G. Shen, J. X. Li, H. J. Lin, S. S. Feng and Y. C. Zhang, *Polym. Bull.*, 2017, **74**, 3639–3655.
16 Y. C. Zhang, J. X. Li, L. G. Shen, H. J. Lin and Y. D. Shan, *J. Appl. Polym. Sci.*, 2017, **134**, 7.
17 R. Sengupta, V. K. Tikku, A. K. Somani, T. K. Chaki and A. K. Bhowmick, *Radiat. Phys. Chem.*, 2005, **72**, 625–633.
18 E. Adem, G. Burillo, L. F. del Castillo, M. Vasquez, M. Avalos-Borja and A. Marcos-Fernandez, *Radiat. Phys. Chem.*, 2014, **97**, 165–171.
19 H. S. Jung, J. I. Park, P.-H. Kang, M. C. Choi, Y.-W. Chang and S. C. Hong, *Polymer*, 2013, **37**, 571–578.
20 M. Aden, G. Otto and C. Duwe, *Int. Polym. Process.*, 2013, **28**, 300–305.
21 B. Li, Z. Wang, K. Wei, T. Shen, C. Yao, H. Zhang, Y. Sheng, X. Lu, A. Xiong and W. Han, *Fusion Eng. Des.*, 2019, **142**, 6–12.
22 X. Xiao, *Metals*, 2019, **9**, 1132.
23 C. Xu, X. Liu, F. Xue, Y. Li and W. Qian, *Nucl. Instrum. Methods Phys. Res., Sect. B*, 2018, **427**, 87–90.
24 Z.-f. Fu, S.-q. Ma and S.-l. Ma, *Chin. J. Cancer*, 2002, **21**, 518–521.
25 A. Kuramoto, T. Toyama, Y. Nagai, K. Inoue, Y. Nozawa, M. Hasegawa and M. Valo, *Acta Mater.*, 2013, **61**, 5236–5246.
26 L. Yue, Y. Wu, C. Sun, J. Xiao, Y. Shi, G. Ma and S. He, *Nucl. Instrum. Methods Phys. Res., Sect. B*, 2012, **291**, 17–21.
27 M. Hidiroglu, D. Aksut, O. Serce, H. Karabulut and M. Sen, *Radiat. Phys. Chem.*, 2019, **159**, 118–123.
28 S. I. S. M. Reffai, T. Chatterjee and K. Naskar, *Radiat. Phys. Chem.*, 2018, **148**, 50–59.
29 Y. Zhao, W. Yu, R. Li, Y. Xu, Y. Liu, T. Sun, L. Shen and H. Lin, *Appl. Surf. Sci.*, 2019, **483**, 1006–1016.
30 W. Yu, Y. Liu, Y. Xu, R. Li, J. Chen, B.-Q. Liao, L. Shen and H. Lin, *J. Membr. Sci.*, 2019, **581**, 401–412.
31 W. Yu, Y. Liu, L. Shen, Y. Xu, R. Li, T. Sun and H. Lin, *Chemosphere*, 2020, **243**, 125446.
32 T. Sun, Y. Liu, L. Shen, Y. Xu, R. Li, L. Huang and H. Lin, *J. Colloid Interface Sci.*, 2020, **570**, 273–285.
33 Y. Li, Y. Song, J. Li, Y. Li, N. Li and S. Niu, *Ultrason. Sonochem.*, 2018, **42**, 18–25.
34 M. Porubska, D. Babic, I. Janigova, M. Slouf, K. Jomova and I. Chodak, *Polym. Bull.*, 2016, **73**, 1775–1794.
35 M. Porubska, I. Janigova, K. Jomova and I. Chodak, *Radiat. Phys. Chem.*, 2014, **102**, 159–166.
36 L. Su, L. Tao, T. Wang and Q. Wang, *Polym. Degrad. Stab.*, 2012, **97**, 981–986.
37 E. Domingos, T. M. C. Pereira, E. V. R. de Castro, W. Romao, G. L. de Sena and R. C. L. Guimaraes, *Polim.: Cienc. Tecnol.*, 2013, **23**, 37–41.
38 S. Deng, Q. Ran, S. Wu and J. Shen, *Polym. Polym. Compos.*, 2008, **16**, 375–378.

Open Access Article. Published on 05 June 2020. Downloaded on 12/4/2025 11:48:17 PM.
This article is licensed under a Creative Commons Attribution-NonCommercial 3.0 Unported Licence.

39 K.-H. Loo, L. T. Sin, S.-T. Bee, C. T. Ratnam, S.-L. Bee, T.-T. Tee and A. R. Rahmat, *Polym. Eng. Sci.*, 2019, **59**, 1017–1027.
40 M. Qiao, S.-S. Wu, J. Shen and Q.-P. Ran, *J. Thermoplast. Compos. Mater.*, 2010, **23**, 137–148.
41 L. Yang, Z. Zhang, X. Wang, J. Chen and H. Li, *J. Appl. Polym. Sci.*, 2013, **128**, 1510–1520.
42 S. Malmir, M. K. R. Aghjeh, M. Hemmati and R. A. Tehrani, *J. Appl. Polym. Sci.*, 2012, **125**, E503–E514.
43 E. Moghbelli, H.-J. Sue and S. Jain, *Polymer*, 2010, **51**, 4231–4237.
44 M. R. Saeb, H. A. Khonakdar, M. Razban, S. H. Jafari, H. Garmabi and U. Wagenknecht, *Macromol. Chem. Phys.*, 2012, **213**, 1791–1802.

 This journal is © The Royal Society of Chemistry 2020